Altered RNA processing and export lead to retention of mRNAs near transcription sites and nuclear pore complexes or within the nucleolus

Biplab Paul and Ben Montpetit*
Department of Cell Biology, University of Alberta, Edmonton, AB T6G 2H7, Canada

ABSTRACT **Many protein factors are required for mRNA biogenesis and nuclear export, which are central to the eukaryotic gene expression program. It is unclear, however, whether all factors have been identified. Here we report on a screen of >1000 essential gene mutants in *Saccharomyces cerevisiae* for defects in mRNA processing and export, identifying 26 mutants with defects in this process. Single-molecule FISH data showed that the majority of these mutants accumulated mRNA within specific regions of the nucleus, which included 1) mRNAs within the nucleolus when nucleocytoplasmic transport, rRNA biogenesis, or RNA processing and surveillance was disrupted, 2) the buildup of mRNAs near transcription sites in 3′-end processing and chromosome segregation mutants, and 3) transcripts being enriched near nuclear pore complexes when components of the mRNA export machinery were mutated. These data show that alterations to various nuclear processes lead to the retention of mRNAs at discrete locations within the nucleus.**

Monitoring Editor
Sandra Wolin
Yale University

Received: Apr 27, 2016
Revised: Jun 23, 2016
Accepted: Jun 29, 2016

INTRODUCTION

Nascent RNA transcripts are processed and mature within the nucleus, including folding, cleavage, modification, nuclear export, or decay. Processing is driven by specific RNA–protein and RNA–RNA interactions that occur in the context of a ribonucleoprotein (RNP) particle, with the protein composition of the RNP being largely responsible for the processing path that is followed (Mitchell and Parker, 2014; Oeffinger and Montpetit, 2015; Singh *et al.*, 2015). In the case of mRNA biogenesis in *Saccharomyces cerevisiae*, cotranscriptional recruitment of capping enzymes, splicing machinery, and various RNA adaptor proteins mediate maturation of the pre-mRNA, which includes cleavage and polyadenylation during 3′-end formation, loading of export receptors (e.g., Mex67p), and release of the messenger ribonucleoprotein (mRNP) from the transcription site (Oeffinger and Zenklusen, 2012; Niño *et al.*, 2013). After release, mRNPs are often exported through nuclear pore complexes (NPCs), which are assembled from ~30 nucleoporins (Nups) to form a transport channel spanning the nuclear envelope (Wente and Rout, 2010). mRNP docking and translocation through an NPC are directed by interactions between Mex67p and other mRNP components with Nups of the nuclear basket and central transport channel (Bonnet and Palancade, 2014). On reaching the cytoplasmic side of the NPC, export is terminated by the action of the DEAD-box ATPase Dbp5p, which is locally activated by the cytoplasmic nucleoporins Nup159p and Gle1p with the small molecule $InsP_6$ (Oeffinger and Zenklusen, 2012; Björk and Wieslander, 2014). This ultimately results in removal of Mex67p, release of mRNP into the cytoplasm, and directionality in mRNA export.

Inevitably, errors occur during nuclear RNA processing, which can result in aberrant transcripts being targeted for nuclear degradation via quality control mechanisms (Houseley and Tollervey, 2009; Müller-McNicoll and Neugebauer, 2013; Eberle and Visa, 2014; Porrua and Libri, 2015). A key player in this process is the exosome, which functions in the nucleus and cytoplasm as a nuclease to facilitate and surveil RNA biogenesis from all three nuclear RNA polymerases (Chlebowski *et al.*, 2013; Porrua and Libri, 2013; Schneider and Tollervey, 2013). The nuclear exosome differs in composition from the cytoplasmic form through the addition of a

This article was published online ahead of print in MBoC in Press (http://www.molbiolcell.org/cgi/doi/10.1091/mbc.E16-04-0244) on July 6, 2016.

*Address correspondence to: Ben Montpetit (ben.montpetit@ualberta.ca).

Abbreviations used: mRNP, messenger ribonucleoprotein; NPC, nuclear pore complex; Nup, nucleoporin; RNP, ribonucleoprotein; smFISH, single-molecule fluorescent in situ hybridization.

second catalytic subunit, Rrp6p (Briggs *et al.*, 1998), which, together with Dis3p, harbors the nuclease activities associated with the exosome. Nine other protein subunits are found within the exosome (Liu *et al.*, 2006), which function to recognize and feed RNA substrates Dis3p and Rrp6p (Bonneau *et al.*, 2009; Malet *et al.*, 2010), mediate interactions with multiple protein complexes that include the TRAMP, NNS, and SKI complexes (Jacobs *et al.*, 1998; Steinmetz *et al.*, 2001; Kadaba *et al.*, 2004; Ursic *et al.*, 2004; LaCava *et al.*, 2005; Vanácová *et al.*, 2005; Wyers *et al.*, 2005; Vasiljeva and Buratowski, 2006), and regulate the overall activity of Dis3p and Rrp6p (Mitchell *et al.*, 1997; Allmang *et al.*, 1999; Wasmuth and Lima, 2012).

Disruptions to RNA biogenesis, export, and surveillance result in the accumulation of aberrant RNP complexes and RNA processing by-products in the nucleus of the affected cell (Amberg *et al.*, 1992; Kadowaki *et al.*, 1992, 1994a; Doye *et al.*, 1994; Fabre *et al.*, 1994; Gorsch *et al.*, 1995; Segref *et al.*, 1997). For example, when exosome-dependent RNA processing and surveillance are perturbed, the biogenesis of small nucleolar RNA (snoRNA), rRNA, tRNA, mRNA, and other noncoding transcripts is altered (van Hoof *et al.*, 2000; Kuai *et al.*, 2004; LaCava *et al.*, 2005; Vanácová *et al.*, 2005; Wyers *et al.*, 2005; David *et al.*, 2006; Davis and Ares, 2006; Houalla *et al.*, 2006; Carneiro *et al.*, 2007; Gudipati *et al.*, 2012; Schneider *et al.*, 2012; Castelnuovo *et al.*, 2013). Such disruptions to RNA biogenesis and export can often be observed as the accumulation of poly(A)-RNA species within the nucleus of the affected cell (Cole *et al.*, 2002), which has been used to identify many mutants involved in RNA biogenesis and export, including screening of the ~5000 nonessential genes in *S. cerevisiae* for mRNA export defects (Hieronymus *et al.*, 2004). The construction of mutant libraries that span essential genes (Ben-Aroya *et al.*, 2008; Breslow *et al.*, 2008; Li *et al.*, 2011) provides an opportunity to conduct comprehensive screens of essential genes for mRNA processing and export defects, as recently performed for tRNA (Wu *et al.*, 2015). Of importance, the screening of both essential (this work) and nonessential (Hieronymus *et al.*, 2004; Thomsen *et al.*, 2008) genes within *S. cerevisiae* for mRNA-processing defects provides a component list that is necessary for building complete models of mRNA biogenesis and export.

Here we report on a screen of largely essential gene mutants for nuclear poly(A)-RNA accumulation and the characterization of these mutants using single-molecule fluorescent in situ hybridization (smFISH) directed against specific mRNAs. This resulted in the identification of 15 genes that were not previously linked and/or demonstrated to alter RNA processing and mRNA export. In addition, disruption of multiple nuclear processes was found to cause distinct phenotypes that included the accumulation of mRNAs near transcription sites or the nuclear periphery and NPCs or within the nucleolus. These data suggest that alterations to RNA processing and overall nuclear homeostasis cause RNAs to stall or be retained at similar restriction points. This may reflect common failures in mRNA biogenesis and export, as well as active mechanisms to protect the cell during cellular stress and dysfunction.

RESULTS

Identification of mutants that accumulate nuclear poly(A)-RNA

To potentially identify genes involved in mRNA biogenesis and export, we screened two temperature-sensitive (*Ts*) *S. cerevisiae* mutant collections (Ben-Aroya *et al.*, 2008; Li *et al.*, 2011) for the accumulation of poly(A)-RNA in the nucleus using an oligo-dT FISH assay. Together these two *Ts* collections cover ~68% (785 of 1156) of essential genes. When a *Ts* allele was not available, a DAmP allele was used that harbors a disrupted 3′ untranslated region often leading to reduced gene expression (Breslow *et al.*, 2008), which increased coverage of essential genes to ~91% (1047 of 1156) in our screen (Supplemental Data). For consistency throughout the screening process, regardless of the type of mutant used, all strains were grown into log phase at 25°C, shifted to 37°C for 3 h, and fixed. A 3-h temperature shift was used to balance the time needed to induce the *Ts* mutant phenotype(s) while minimizing induction of secondary phenotypes caused by the loss of essential cellular activities. In the case of the DAmP alleles, it was reasoned that the temperature shift might act as a stress and exacerbate mutant phenotypes, although DAmP alleles are not necessarily *Ts* mutants. After fixation, we performed in situ assays using a fluorescently labeled oligo-dT probe to detect poly(A)-RNA.

By comparing the distribution of oligo-dT to the 4′,6-diamidino-2-phenylindole (DAPI) signal, we identified 29 of 1047 mutants that accumulated poly(A)-RNA in the nucleus (Supplemental Figure S1 and Table 1). Of the genes identified, only half (14 of 29) were previously reported to display nuclear accumulation of poly(A)-RNA when disrupted (Table 1). To verify that the poly(A)-RNA accumulation phenotype was linked to the purported mutant being screened, we verified all strains by PCR, and in the case of the 15 newly reported genes, the mutation was rescued by introducing a wild-type allele and/or recapitulated by moving the mutation to a different strain background (Table 1). Note that not all genes previously reported to accumulate poly(A)-RNA in the nucleus when disrupted were identified by our screen, which may be due to the specific allele present in the mutant collection, the length of the temperature shift, or the requirement of a poly(A) tail for detection in the initial in situ screen. Within the set of mutants identified, the distribution of poly(A)-RNA within the nucleus was distinct and included bright foci (*brl1-3231*), a diffuse nuclear signal (*rsp5-3*), a diffuse nuclear signal with one or more foci (*dbp5-1*), or poly(A)-RNA being adjacent to the DAPI-stained DNA mass (*dis3-1*; Figure 1A). The pattern of poly(A)-RNA accumulation was similar for genes with related biological functions (e.g., RNA processing and surveillance, with an accumulation of poly(A)-RNA next to DAPI; Table 1), which supports the notion that these mutants affect RNA biogenesis in distinct ways and the localization pattern can be informative for gene function.

Nucleolar disruption is linked to poly(A)-RNA accumulation

Studies in *Schizosaccharomyces pombe* have shown that mutants affecting chromosome biology are associated with the accumulation of nuclear poly(A)-RNA and nucleolar disruption (Kalam Azad *et al.*, 2003; Ideue *et al.*, 2004). Of the genes identified in our screen, approximately one-third have functions that include kinetochore–microtubule attachment, chromosome organization, and cell cycle checkpoint control (Table 1). Given these facts and the reported defects in rDNA segregation within mutants identified here (e.g., *IPL1* and *SMC* genes; Freeman, 2000; D'Amours *et al.*, 2004; Sullivan *et al.*, 2004; Machín *et al.*, 2005), we assayed nucleolar status in all 29 mutants based on the rRNA-processing intermediate (*ITS1*) and nucleolar protein (Nop56p–green fluorescent protein [GFP]; Gautier *et al.*, 1997; Woolford and Baserga, 2013). By monitoring each nucleolar marker and poly(A)-RNA in the same cell, we found that 21 of the 29 mutants displayed alterations in *ITS1* and/or Nop56p-GFP localization and abundance when poly(A)-RNA accumulated (Table 1), which included fragmented nucleoli in mRNA export mutants, as previously reported (Kadowaki *et al.*, 1994b; Dockendorff *et al.*, 1997; Segref *et al.*, 1997; Thomsen *et al.*, 2008). Nucleolar disruption was prominent in seven of the nine mutants

Gene	Biological process	Previous report/ verification[a]	Distribution of nuclear poly(A)-RNA	Cells with nuclear poly(A)-RNA accumulation ± SD (%)	*GFA1* mRNAs per cell ± SD	Nuclear *GFA1* mRNAs[b]	*ITS1* and Nop56-GFP
URA10	Pyrimidine biosynthesis	–	Diffuse	<1	5.1 ± 0.7	0.9 ± 0.9 (1)	–
ALR1	Plasma membrane Mg^{2+} transporter	Rescued	Foci	36 ± 2	11.1 ± 1.7	1.8 ± 1.6* (1)	–
BRL1	NPC and nuclear envelope biogenesis	Saitoh *et al.* (2005)	Diffuse signal/ foci	34 ± 11	6.0 ± 0.6	1.3 ± 1.1* (1)	–
BRR6	NPC and nuclear envelope biogenesis	de Bruyn Kops and Guthrie (2001)	Diffuse signal/ foci	49 ± 4	4.5 ± 1.1	1.1 ± 1.0* (1)	–
CBF2	Chromosome segregation	Rescued	Diffuse signal/ foci	27 ± 11	5.2 ± 1.2	0.9 ± 0.9 (1)	Both absent in cells with nuclear poly(A)-RNA
CEP3	Chromosome segregation	Rescued	Diffuse signal/ foci	16 ± 4	6.7 ± 0.9	1.0 ± 1.3 (1)	Both absent in cells with nuclear poly(A)-RNA
CLP1	Cleavage and polyadenylation of RNA	Rescued	Foci	32 ± 10	9.6 ± 1.3	1.6 ± 1.3* (1)	Nop56-GFP foci
CSL4	RNA processing and degradation	Remade	Diffuse signal next to DAPI	~100	6.0 ± 1.9	2.3 ± 1.9* (2)	Enlarged ITS1 and Nop56-GFP area
DBP5	RNA export	Snay-Hodge *et al.* (1998), Tseng *et al.* (1998)	Diffuse signal/ foci	~100	4.2 ± 0.3	2.2 ± 1.5* (2)	ITS1 and Nop56-GFP foci
DIS3	RNA processing/ degradation	Kadowaki *et al.* (1994a)	Diffuse signal next to DAPI	~100	5.5 ± 1.0	2.1 ± 1.5* (2)	Enlarged ITS1 and Nop56-GFP area
ENP1	RNA processing and ribosomal subunit synthesis	Rescued	Diffuse signal next to DAPI	~100	3.4 ± 0.5	2.0 ± 1.5* (2)	ITS1 decreased or absent
GLE1	RNA export	Del Priore *et al.* (1996), Murphy and Wente (1996)	Diffuse signal/ foci	~100	2.2 ± 0.3	2.1 ± 1.3* (2)	ITS1 and Nop56-GFP foci
IPL1	Chromosome segregation/cell cycle	Cole *et al.* (2002)	Diffuse signal/ foci	30 ± 12	3.4 ± 0.5	0.8 ± 0.9 (1)	Both absent in cells with nuclear poly(A)-RNA
LDB19	Ubiquitin-dependent endocytosis	Remade	Diffuse signal	17 ± 3	6.2 ± 0.5	0.9 ± 1.0 (1)	–
MEX67	RNA export	Segref *et al.* (1997)	Diffuse signal/ foci	~100	2.4 ± 0.6	2.1 ± 1.2* (2)	ITS1 and Nop56-GFP foci

TABLE 1: Description and phenotypes associated with mutants that display poly(A)-RNA accumulation.

Continues

Gene	Biological process	Previous report/ verification[a]	Distribution of nuclear poly(A)-RNA	Cells with nuclear poly(A)-RNA accumulation ± SD (%)	*GFA1* mRNAs per cell ± SD	Nuclear *GFA1* mRNAs[b]	*ITS1* and Nop56-GFP
MPS1	Spindle pole body/ cell cycle	Rescued	Diffuse signal/ foci	28 ± 4	6.5 ± 1.2	1.1 ± 1.1 (1)	Both absent in cells with nuclear poly(A)-RNA
MTR4	RNA processing and surveillance	Kadowaki *et al.* (1994a)	Diffuse signal next to DAPI	~100	4.9 ± 0.7	2.3 ± 1.5* (2)	ITS1 decreased or absent
NUP133	Nucleocytoplasmic transport	Doye *et al.* (1994)	Diffuse signal/ foci	59 ± 5	5.7 ± 0.8	1.3 ± 1.0* (1)	–
NUP145	Nucleocytoplasmic transport	Fabre *et al.* (1994), Wente and Blobel (1994)	Diffuse signal/ foci	43 ± 2	4.6 ± 0.6	1.2 ± 1.0* (1)	–
NUP159	Nucleocytoplasmic transport	Gorsch *et al.* (1995)	Diffuse signal/ foci	~100	1.7 ± 0.2	1.6 ± 1.0* (1)	ITS1 and Nop56-GFP foci
PRP2	Pre-mRNA splicing	Rescued	Diffuse signal	34 ± 12	5.9 ± 0.5	1.1 ± 1.1 (1)	–
PTA1	Cleavage and polyadenylation of RNA	Hammell *et al.* (2002)	Diffuse signal/ foci	35 ± 8	6.1 ± 0.9	1.2 ± 1.0* (1)	–
RRP43	RNA processing and degradation	Rescued	Diffuse signal next to DAPI	~100	5.3 ± 0.3	1.8 ± 1.7* (1)	Enlarged ITS1 and Nop56-GFP area
RSP5	E3 ubiquitin ligase; multiple processes	Neumann *et al.* (2003), Rodriguez *et al.* (2003)	Diffuse signal	~100	5.7 ± 2.0	1.2 ± 0.9* (1)	–
SLI15	Chromosome segregation/cell cycle	Remade	Diffuse signal/ foci	30 ± 4	4.9 ± 1.1	1.0 ± 1.2 (1)	Both absent in cells with nuclear poly(A)-RNA
SMC1	Chromosome segregation	Rescued	Diffuse signal/ foci	14 ± 2	4.3 ± 0.5	1.0 ± 1.2 (1)	–
SMC3	Chromosome segregation	Rescued	Diffuse signal/ foci	51 ± 13	5.7 ± 0.3	1.3 ± 1.2* (1)	–
SMC4	Chromosome organization	Rescued	Diffuse signal/ foci	29 ± 7	9.0 ± 2.5	1.1 ± 1.3 (1)	Both absent in cells with nuclear poly(A)-RNA
SPC24	Chromosome segregation	Remade	Diffuse signal/ foci	33 ± 6	4.3 ± 1.1	0.9 ± 1.1 (1)	Both absent in cells with nuclear poly(A)-RNA
SRM1/ PRP20	Nucleocytoplasmic transport	Amberg *et al.* (1993), Kadowaki *et al.* (1994a)	Diffuse signal next to DAPI	~100	2.1 ± 0.2	0.6 ± 0.7* (0)	ITS1 decreased or absent

[a]To verify mutants that had not previously been reported to accumulate poly(A)-RNA, the phenotype was rescued using a wild-type allele or recapitulated by making the mutant in a different strain background as indicated.

[b]Average number of nuclear mRNAs ± SD with the median for the data shown in parentheses.

*Distribution of nuclear mRNAs tested using the Wilcoxon-rank sum test and found to be significant at $p < 0.001$.

TABLE 1: Description and phenotypes associated with mutants that display poly(A)-RNA accumulation. Continued

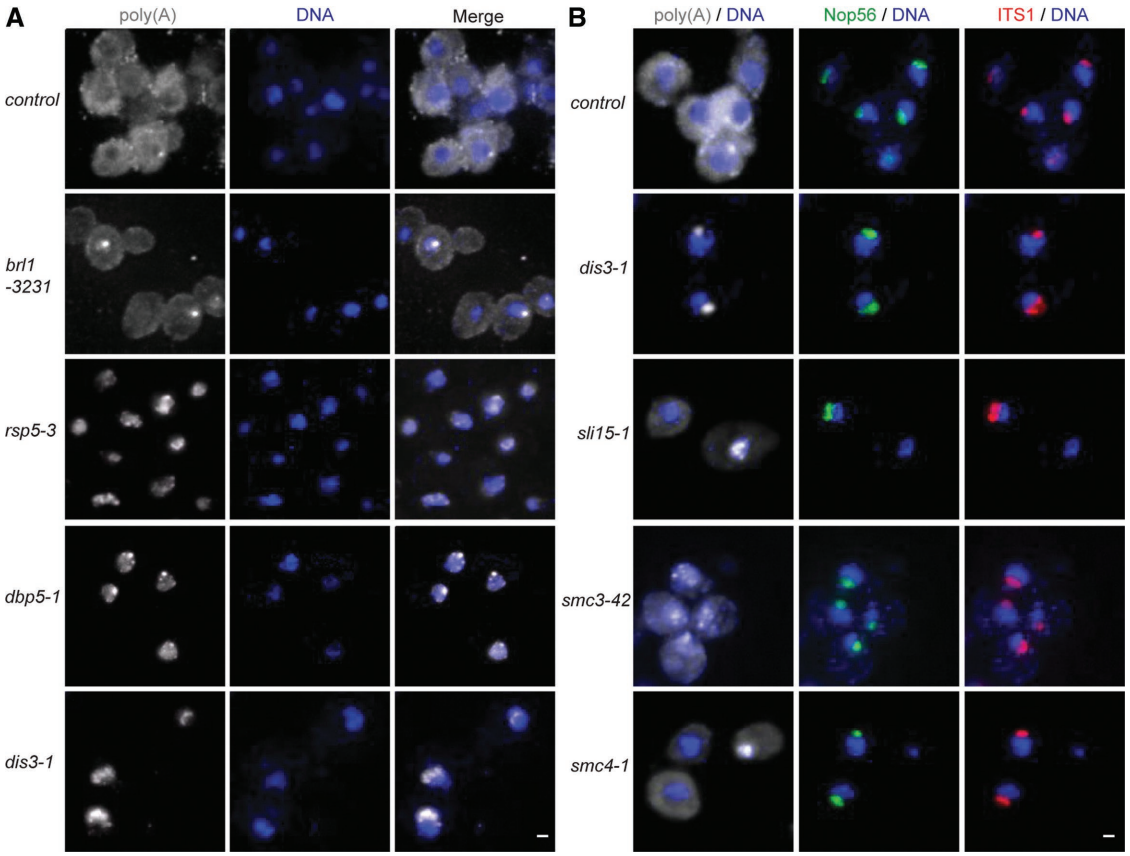

FIGURE 1: Poly(A)-RNA localization patterns and nucleolar status. (A) Representative images showing poly(A)-RNA (gray) localization in control (*ura10*Δ) and select mutant strains compared with DAPI (blue) after 3 h at 37°C. (B) Representative images showing poly(A)-RNA (gray) localization in control (*ura10*Δ) and select mutant strains compared with DAPI (blue), Nop56p-GFP (green), and *ITS1* (red) after 3 h at 37°C. Scale bars, 1 μm.

that affect chromosome biology, with these mutants often lacking nucleolar *ITS1* and Nop56p-GFP in cells with poly(A)-RNA accumulation (e.g., *sli15-1* and *smc4-1* vs. *dis3-1*; Figure 1B). Although *SMC1* and *SMC3* mutants did not show obvious nucleolar defects, recent reports provide a direct role for cohesins (e.g., *SMC3*) in nucleolar function (Bose *et al.*, 2012; Harris *et al.*, 2014). Together these findings further support a link between poly(A)-RNA accumulation and alterations to the nucleolus, which may often be induced by errors in chromosome segregation.

Identification of mRNA biogenesis and export mutants

Mutations within RNA processing and surveillance pathways have been shown to accumulate poly(A)-RNA species, including rRNA, mRNA, snRNA, snoRNA, and tRNA (van Hoof *et al.*, 2000; Kuai *et al.*, 2004; LaCava *et al.*, 2005; Vanácová *et al.*, 2005; Wyers *et al.*, 2005; Carneiro *et al.*, 2007; Rougemaille *et al.*, 2007; Gudipati *et al.*, 2012; Schneider *et al.*, 2012; Castelnuovo *et al.*, 2013). Consequently the mutants identified here using an oligo-d(T)–based in situ approach may accumulate poly(A)-RNA due to disruptions in RNA biogenesis that are independent of mRNA. To identify those mutants that alter mRNA processing and export, we performed smFISH assays using probes against *GFA1*, *ACT1*, or *CCW12* transcripts. The mRNAs were selected based on relative expression levels (*GFA1* = low and *ACT1*/*CCW12* = high) and the presence of an intron in *ACT1* (Ng and Abelson, 1980) that may lead to this mRNA being affected differently than nonspliced mRNAs (i.e., *CCW12* and *GFA1*). To ensure that a block in mRNA export could be observed, we used a *mex67-5* strain, which, when shifted to the nonpermissive temperature, rapidly accumulated poly(A)-RNA in the nucleus (Segref *et al.*, 1997). smFISH assays using the gene-specific probes displayed an obvious block in mRNA export at the nonpermissive temperature in *mex67-5*, and, of importance, a *mex67-5*/*ccw12*Δ strain showed no detectable signal with the *CCW12* probe set (Figure 2A). This established that these mRNA probes can be used to detect export defects, and in the case of CCW12, the probes were specific for the transcript being targeted.

Using smFISH data for *GFA1*, we determined the number of transcripts and distribution of these transcripts between the nucleus and cytoplasm. In a haploid control strain (*ura10*Δ), *GFA1* was found to be present at approximately five copies per cell, with ~18% of these transcripts being in the nucleus (based on DAPI and ITS1 signals), whereas the mRNA export mutant *mex67-5* contained ~88% of transcripts in the nucleus (Table 1 and Figure 2A). Most mutants showed less than a twofold change in *GFA1* levels, with nuclear pools of the mRNA that varied between 16 and 95% (Table 1). In the case of *prp2-1*, there was no effect on *GFA1* localization or transcript number, but *ACT1* export was altered (Figure 2B), which is consistent with the role of Prp2p in splicing (Lustig *et al.*, 1986). For *brl1-3231* and *brr6-ph*, these mutants showed no mRNA export defect after a 3-h temperature shift, but given the role of the gene products in nuclear envelope maintenance and NPC biogenesis (de Bruyn Kops and Guthrie, 2001; Saitoh *et al.*, 2005; Hodge *et al.*, 2010;

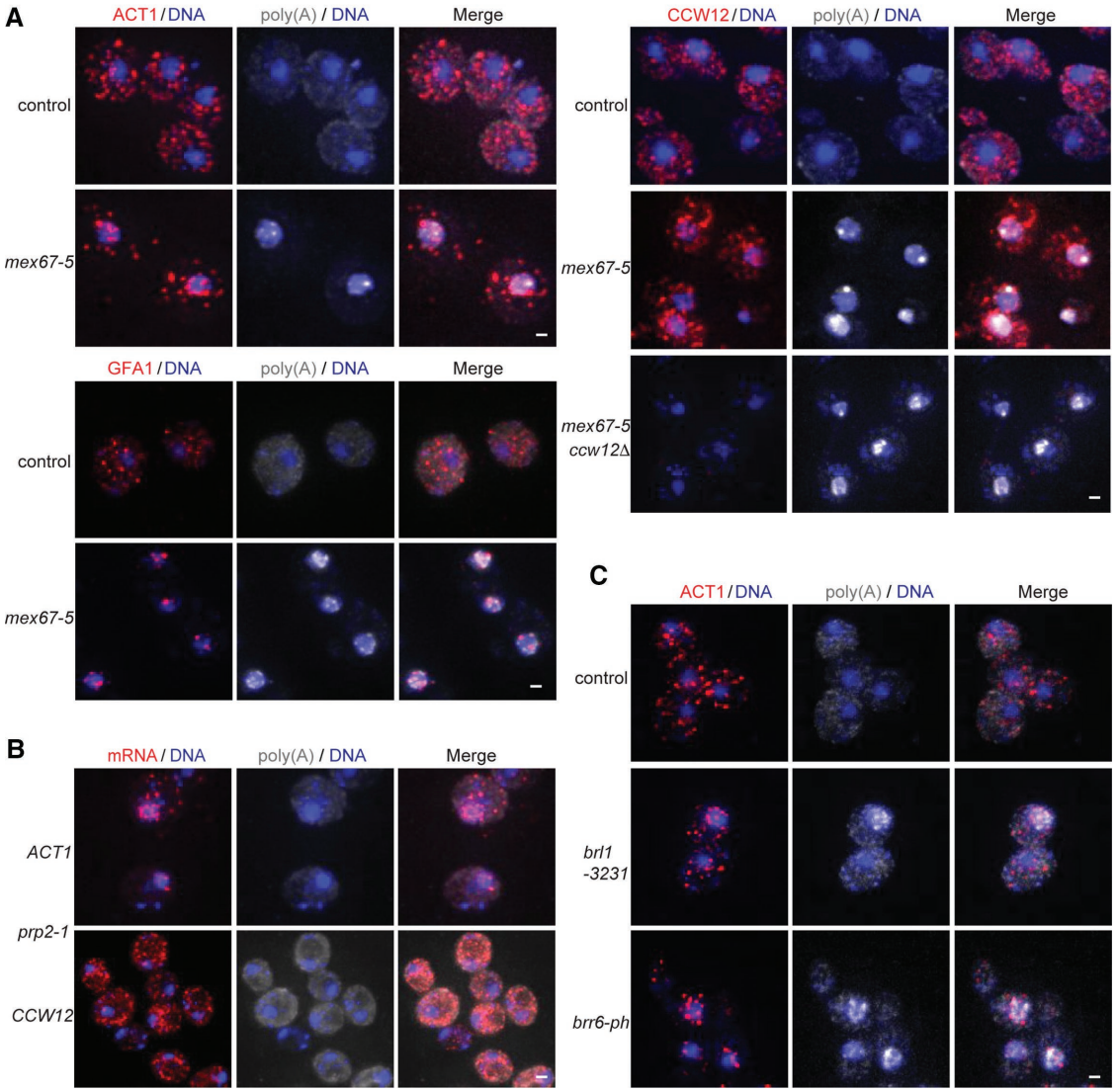

FIGURE 2: Identification of mRNA export mutants using smFISH. (A) Representative images showing *ACT1*, *GFA1*, or *CCW12* mRNA (red) localization in control (*ura10*Δ), *mex67-5*, or *mex67-5/ccw12*Δ strains compared with poly(A)-RNA (gray) and DAPI (blue) after 3 h at 37°C. (B) Representative images showing *ACT1* or *CCW12* mRNA (red) localization in the *prp2-1* strain compared with poly(A)-RNA (gray) and DAPI (blue) after 3 h at 37°C. (C) Representative images showing *ACT1* mRNA (red) localization in control (*ura10*Δ), *brl1-3231*, and *brr6-ph* strains compared with poly(A)-RNA (gray) and DAPI (blue) after 6 h at 37°C. Scale bars, 1 μm.

Lone *et al.*, 2015), we expected to observe a defect. We performed a 6-h temperature shift, providing additional time for *Ts* phenotypes to develop, and under these conditions, we observed mRNA export defects for both mutants (Figure 2C).

mRNAs localize to distinct subdomains of the nucleus in mutants

smFISH data showed that some mutants had a large increase in the fraction of nuclear mRNAs (e.g., *mex67-5* and *gle1-4*), whereas others did not (e.g., *rsp5-3* and *sli15-1*). However, in almost all instances, the localization of mRNAs appeared distinct in the mutants tested (Supplemental Data). For example, strains carrying mutations in genes directly linked to the mRNA export process (e.g., *DBP5, GLE1, MEX67*, and *NUP159)* often had mRNAs near the periphery of the DAPI-stained DNA mass (see *mex67-5* in Figure 2). This suggests that within these mutants, mRNAs accumulated at or near nuclear pore complexes, as reported for mutants of *MEX67* (Hurt *et al.*, 2000; Smith *et al.*, 2015) and *DBP5* (Hodge *et al.*, 2011). The *prp2-1* mutant also showed *ACT1* transcripts near the nuclear periphery (Figure 2B), which may be related to quality control mechanisms that block export of pre-mRNAs (Galy *et al.*, 2004; Palancade *et al.*, 2005; Iglesias *et al.*, 2010; Hackmann *et al.*, 2014). Using Ndc1p-GFP as a marker of NPCs and the nuclear periphery, we quantified the percentage of transcripts within ~250 nm of the NPC signal in individual cells (n = 50) of select mutants. In control cells, 38 ± 15% of *GFA1* mRNAs were found within this distance, which increased in mRNA export mutants to 68 ± 35% (*mex67-5*) and 61 ± 27% (*dbp5-1*) (Figure 3A). The prp2-1 mutant did not show an increase in peripheral localization of *GFA1* (39 ± 18%), whereas *ACT1* increased from 25 ± 12% in control to 49 ± 17% in prp2-1 (Figure 3B). These data are consistent with the accumulation or retention of mRNAs near NPCs when splicing or late steps in the mRNA export pathway are disrupted.

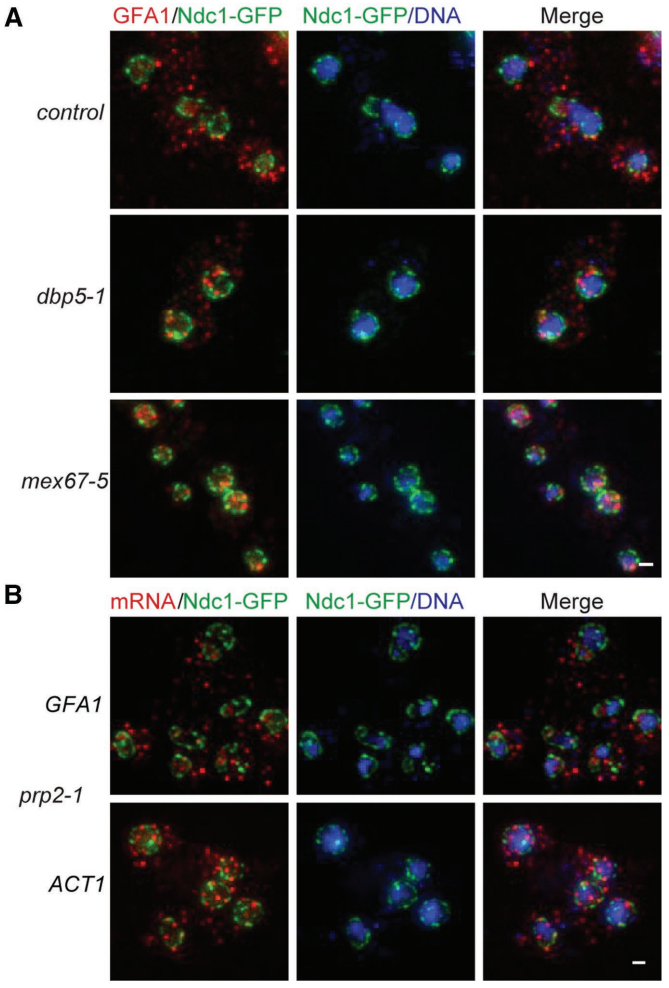

FIGURE 3: Accumulation of mRNA near the nuclear periphery and NPCs. (A) Representative images showing *GFA1* mRNA (red) localization in control (*ura10Δ*), *dbp5-1*, and *mex67-5* strains compared with NPCs (green, Ndc1p-GFP) and DAPI (blue) after 3 h at 37°C. (B) Representative images showing *GFA1* or *ACT1* mRNA (red) localization in the *prp2-1* strain compared with NPCs (green, Ndc1p-GFP) and DAPI (blue) after 3 h at 37°C. Scale bars, 1 μm.

A second distinct localization pattern was the accumulation of mRNAs within a nuclear focus. Rarely present in the control strain, 15 mutants showed >5-fold increase in the frequency of nuclear foci with an intensity ≥10-fold that of single transcripts (Supplemental Data), including *rsp5-3* (Figure 4A). In quantifying the GFA1 smFISH data, we counted such foci as single mRNAs (see *Material and Methods*, *Gene-specific FISH*), which likely underestimates the number of nuclear transcripts in these mutants and leads to a lower level of nuclear accumulation reported in Table 1. Rsp5p is a ubiquitin-ligase that functions in both the cytoplasm and nucleus (Belgareh-Touzé *et al.*, 2008; Kaliszewski and Zoładek, 2008) and has a known role in mRNA biogenesis via modification of the THO/TREX complex (Neumann *et al.*, 2003; Rodriguez *et al.*, 2003; Gwizdek *et al.*, 2005). Given the functions of Rsp5p and other genes with this phenotype, the finding that various mRNA probes show the same defect (i.e., not related to splicing), and the intensity of the smFISH signal, we speculated that these foci represent gene transcription sites.

To test this possibility, we integrated a lacO array ~400 base pairs upstream of the *ACT1* gene, which could be used in combination with LacI-GFP and FISH probes to localize both the *ACT1* gene and mRNA focus. In *rsp5-3*, bright *ACT1* mRNA foci were in close proximity to the ACT1 gene locus, separated by an average distance of 0.15 ± 0.05 μm, whereas the CCW12 mRNA focus was distinct from the *ACT1* gene locus at an average distance of 0.81 ± 0.27 μm (n = 50; Figure 4B). These data are consistent with these bright mRNA foci being at or near transcription

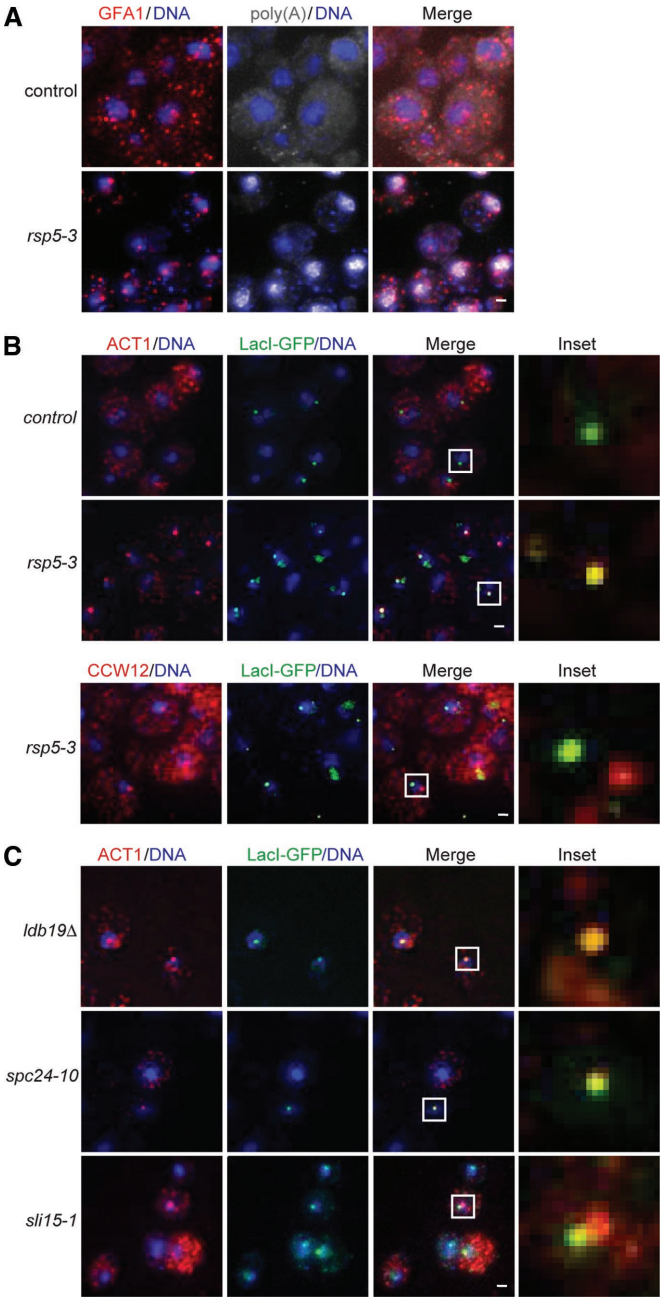

FIGURE 4: Accumulation of ACT1 mRNA near transcription sites. (A) Representative images showing *GFA1* mRNA (red) localization in control (*ura10Δ*) and *rsp5-3* strains compared with poly(A)-RNA (gray) and DAPI (blue) after 3 h at 37°C. (B, C) Representative images showing *ACT1* or *CCW12* mRNA (red) localization in control (*ura10Δ*), *rsp5-3*, *ldb19Δ*, *spc24-10*, and *sli15-1* strains compared with the *ACT1* gene locus (green, marked by lacO-array/GFP-LacI) and DAPI (blue) after 3 h at 37°C. Inset, zoomed-in view of boxed region in the merged image. Scale bars, 1 μm.

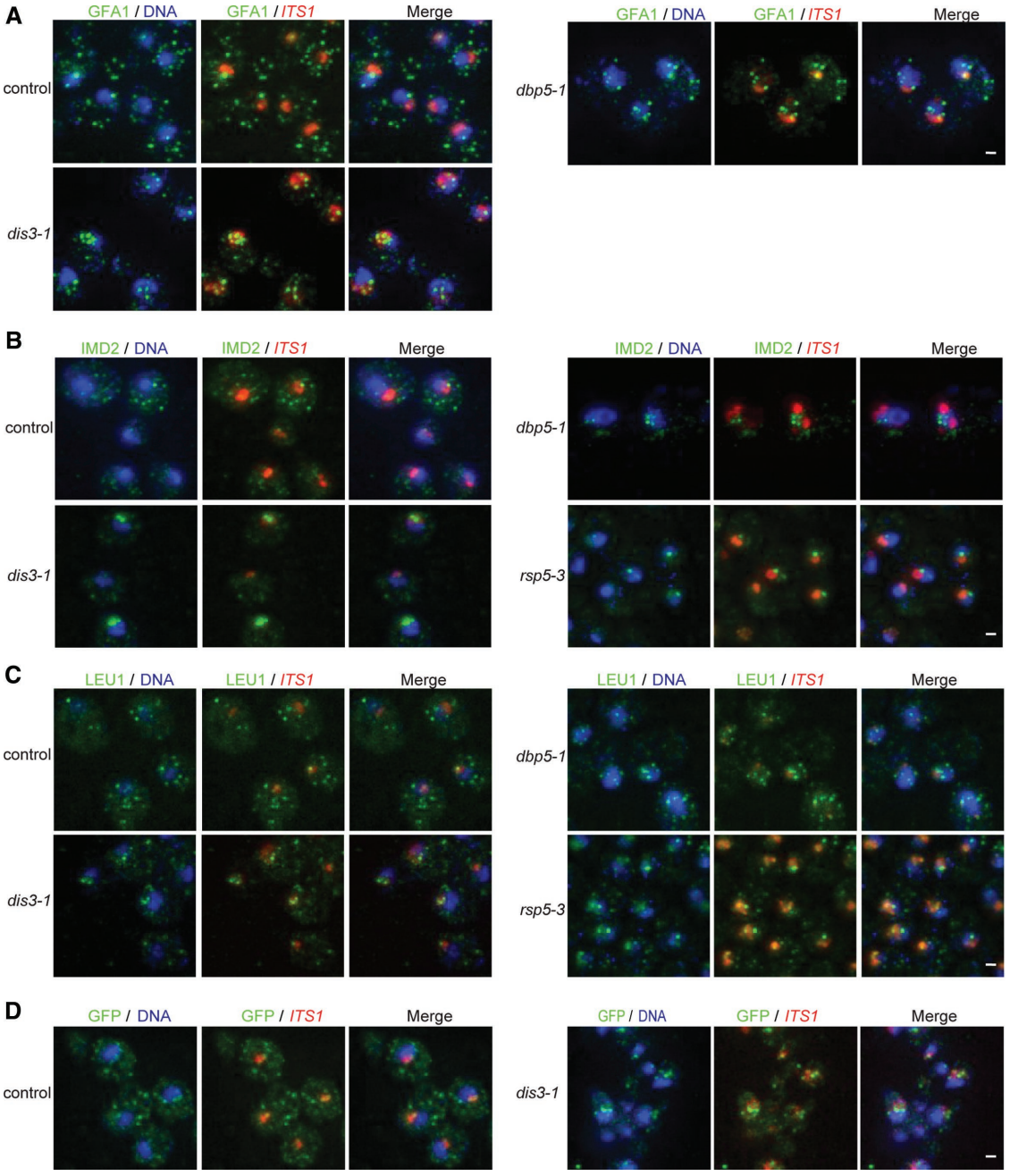

FIGURE 5: Nucleolar localization of mRNA. (A–C) Representative images showing *GFA1*, *IMD2*, or *LEU1* mRNA (green) localization in control (*ura10*Δ), *dbp5-1*, *dis3-1*, and *rsp5-3* strains compared with *ITS1* (red) and DAPI (blue) after 3 h at 37°C. (D) Representative images showing localization of *NAB2-GFP* transcripts using GFP in situ probes (green) in control (*ura10*Δ) and *dis3-1* strains compared with *ITS1* (red) and DAPI (blue) after 3 h at 37°C. Scale bars, 1 μm.

sites. We also observed close association between the *ACT1* mRNA and gene loci in mutants linked to chromosome segregation (*spc24-10* and *sli15-3*), as well as *ldb19*Δ (Figure 4C). Ldb19p is a regulator of Rsp5p that functions in ubiquitin-dependent receptor endocytosis (Lin *et al.*, 2008) but is not known to have a nuclear role. These data match previous reports of mRNAs being retained near transcription sites in THO/TREX complex and mRNA export pathway mutants after heat shock (Hilleren *et al.*, 2001; Jensen *et al.*, 2001; Libri *et al.*, 2002). Moreover, these results demonstrate that the retention of mRNAs at or near transcription sites is a phenotype shared by a set of mutants with diverse cellular functions.

The third localization pattern was an accumulation of mRNAs next to the DAPI-stained DNA mass with or near *ITS1* (Table 1). This included mutants in components of the exosome (e.g., *DIS3*, *RRP43*, and *CSL4*) and TRAMP complex (*MTR4*), which have been reported to accumulate poly(A)-RNA in the nucleolus, as well as the heat shock–induced transcript SSA4 and the localized mRNA ASH1 (Brodsky and Silver, 2000; Thomsen, 2003; Carneiro *et al.*, 2007; Rougemaille *et al.*, 2007; Du *et al.*, 2008). To quantify nucleolar localization (defined by *ITS1* staining), we compared FISH data for *GFA1* between the mRNA export factor (*dbp5-1*) and exosome component (*dis3-1*), which both accumulated *GFA1* transcripts in the nucleus after temperature shift (Figure 5A). Using these data, we

quantified where nuclear mRNA localized with respect to the *ITS1* signal and found 0.4 ± 0.6 and 0.8 ± 0.9 GFA1 transcripts in the nucleolus of the control (*ura10*Δ) and *dbp5-1* strains, respectively. This corresponds to 46% (*ura10*Δ) and 36% (*dbp5-1*) of total nuclear transcripts in these strains (Table 1). In contrast, 1.7 ± 1.2 GFA1 mRNAs were found in the nucleolus of a *dis3-1* strain, which was 80% of the total transcripts in the nucleus of this mutant. This suggests that disruption of exosome function leads to the accumulation of mRNAs within the nucleolus, which is not a general result of mRNAs being retained in the nucleus.

mRNAs can be classified based on protein-binding profiles, which have been used to define 10 general mRNP classes (Tuck and Tollervey, 2013). These range from mRNAs most likely to be processed and exported to the cytoplasm for translation (class X) to those that have protein-binding patterns similar to CUTs (class I), with CUTs being targets of nuclear RNA surveillance (Wyers *et al.*, 2005). The three transcripts we observed in the nucleolus (*GFA1*, *ACT1*, and *CCW12*) belong to class X, and so to extend our observations to other mRNA classes, we used gene-specific FISH probes to assay the localization of *IMD2* (class I) and *LEU1* (class II) mRNAs. In both cases, we observed that these mRNAs were retained in the nucleus of a *dbp5-1* mutant, localized to the nucleolus in *dis3-1*, and appeared as a bright nuclear focus in *rsp5-3* (Figure 5, B and C). By using strains carrying *NAB2-GFP* and GFP FISH probes, we also observed mRNAs within the nucleolus of a *dis3-1* strain (Figure 5D). This implies that mRNAs in the nucleolus are near full length and not short transcripts resulting from early transcription termination, since the GFP probes are directed against the 3′ end of the transcript. These data demonstrate that various mRNAs localize to distinct subdomains of the nucleus when RNA processing and surveillance pathways are disrupted.

mRNP-associated factors are sequestered in the nucleolus with mRNA

After the observation that mRNAs accumulated in the nucleolus, we characterized the subcellular localization of three proteins involved in mRNA processing. Specifically, in control (ura10Δ), *dbp5-1*, and *dis3-1* strains, we assayed localization of Nab2p-GFP (polyadenosine RNA-binding adaptor protein for Mex67p), Prp19p-GFP (splicing factor), and Hrp1p-GFP (subunit of cleavage factor I; required for the cleavage and polyadenylation of mRNA 3′ ends). In control and *dbp5-1* strains, these proteins colocalized with the DAPI-stained DNA mass and were largely absent from the nucleolus as marked by *ITS1* (Figure 6, A–C). In contrast, within the *dis3-1* strain, these factors were found throughout the nuclear volume within both the DAPI- and ITS1-stained regions, suggesting that factors involved in mRNA biogenesis redistribute to the nucleolus in this mutant, similar to mRNAs.

We further tested whether loss of Rrp6p activity would lead to the relocalization of these same factors. Rrp6p is a nonessential catalytic subunit of the exosome that, when mutated, results in poly(A)-RNA accumulation in a discrete domain within the nucleolus (Hieronymus *et al.*, 2004; Carneiro *et al.*, 2007; Rougemaille *et al.*, 2007). In an *rrp6*Δ strain. we observed approximately five GFA1 transcripts per cell, with 18% being nuclear, which is comparable to the control strain (Table 1), but 71% of these nuclear transcripts colocalized with *ITS1* as compared with 46% in control. Nab2p-GFP, Prp19p-GFP, and Hrp1p-GFP were also enriched within the nucleolus (Figure 6, A–C), demonstrating that both mRNA- and mRNP-associated factors are redistributed within the nucleus of an *rrp6*Δ strain.

In addition to mutations in exosome or TRAMP complex components, mutations in *ENP1* and *SRM1* caused accumulation of poly(A)-RNA next to the DAPI-stained DNA mass (Figure 6D and Table 1). Enp1p functions in pre-rRNA processing and 40S subunit synthesis, and Srm1p facilitates nucleocytoplasmic trafficking (Tachibana *et al.*, 1994; Koepp *et al.*, 1996; Chen *et al.*, 2003). *GFA1* mRNAs could be readily observed with the poly(A)-RNA signal that is adjacent to DAPI in both *enp1-1* and *srm1-ts* strains (Figure 6D), but *ITS1* expression was severely reduced in both mutants, preventing us from quantifying *GFA1* localization. Nab2p-GFP, Prp19p-GFP, and Hrp1p-GFP were also localized to the nucleolus of the *enp1-1* strain (Figure 6E); however, *srm1-ts* could not be characterized due to defects in nuclear protein import. These findings demonstrate that localization of mRNAs and mRNP-associated proteins to the nucleolus does not occur only when RNA surveillance and quality control machinery is mutated and can occur as a result of disruption to other nuclear processes.

DISCUSSION

mRNA biogenesis involves the interaction of numerous protein factors with each mRNA in a spatially and temporally regulated manner within the nucleus to link the processes of transcription, capping, splicing, 3′-end formation, RNA surveillance, and NPC-mediated export (Oeffinger and Zenklusen, 2012; Niño *et al.*, 2013). Nuclear events also act to define the fate of each mRNP, which can include marking mRNPs in the nucleus for translation, storage, transport, or decay within the cytoplasm (Müller-McNicoll and Neugebauer, 2013; Singh *et al.*, 2015). Consequently the proper and efficient coordination of these nuclear events is central to the fidelity of the gene expression program, with previous work having identified factors involved in these processes through analysis of individual mutants, genetic screens and comprehensive screening of nonessential genes (Shiokawa and Pogo, 1974; Amberg *et al.*, 1992; Kadowaki *et al.*, 1992, 1994a; Doye *et al.*, 1994; Fabre *et al.*, 1994; Gorsch *et al.*, 1995; Hieronymus *et al.*, 2004). However, the critical nature of these events dictates that essential genes would likely be involved in this process, which prompted us to perform a screen of essential genes for function(s) related to mRNA biogenesis in *S. cerevisiae*. This led to the identification of 29 genes with a nuclear poly(A)-RNA accumulation phenotype (Table 1), of which half (15 of 29) had not previously been reported to have such a defect. Of these, 26 genes were subsequently found to alter mRNA biogenesis and export when mutated, based on the observed accumulation of mRNA in the nucleus and/or altered localization of nuclear mRNAs.

Classes of mRNA biogenesis and export mutants

Gene ontology places the majority of the 29 genes into three biological processes: RNA export from nucleus, nuclear RNA catabolic processes, and chromosome segregation. The identification of mRNA export factors is expected and validates our screen. Links between mRNA export and RNA decay are also well established (Porrua and Libri, 2013; Eberle and Visa, 2014), with various components of the decay machinery having originally been identified in screens for mRNA transport (MTR) mutants (Kadowaki *et al.*, 1992, 1994a). Beyond the related biological functions of the gene products, 26 of the 29 mutants could be further classified into three distinct groups (referred to as class A, B, or C) based on shared phenotypes with respect to the localization of poly(A)-RNA and mRNA within the nucleus (Supplemental Data).

Class A mutants are represented by genes directly involved in mRNA export and NPC function (e.g., *DBP5* and *NUP159*) and were characterized by a diffuse nuclear poly(A)-RNA signal (with or

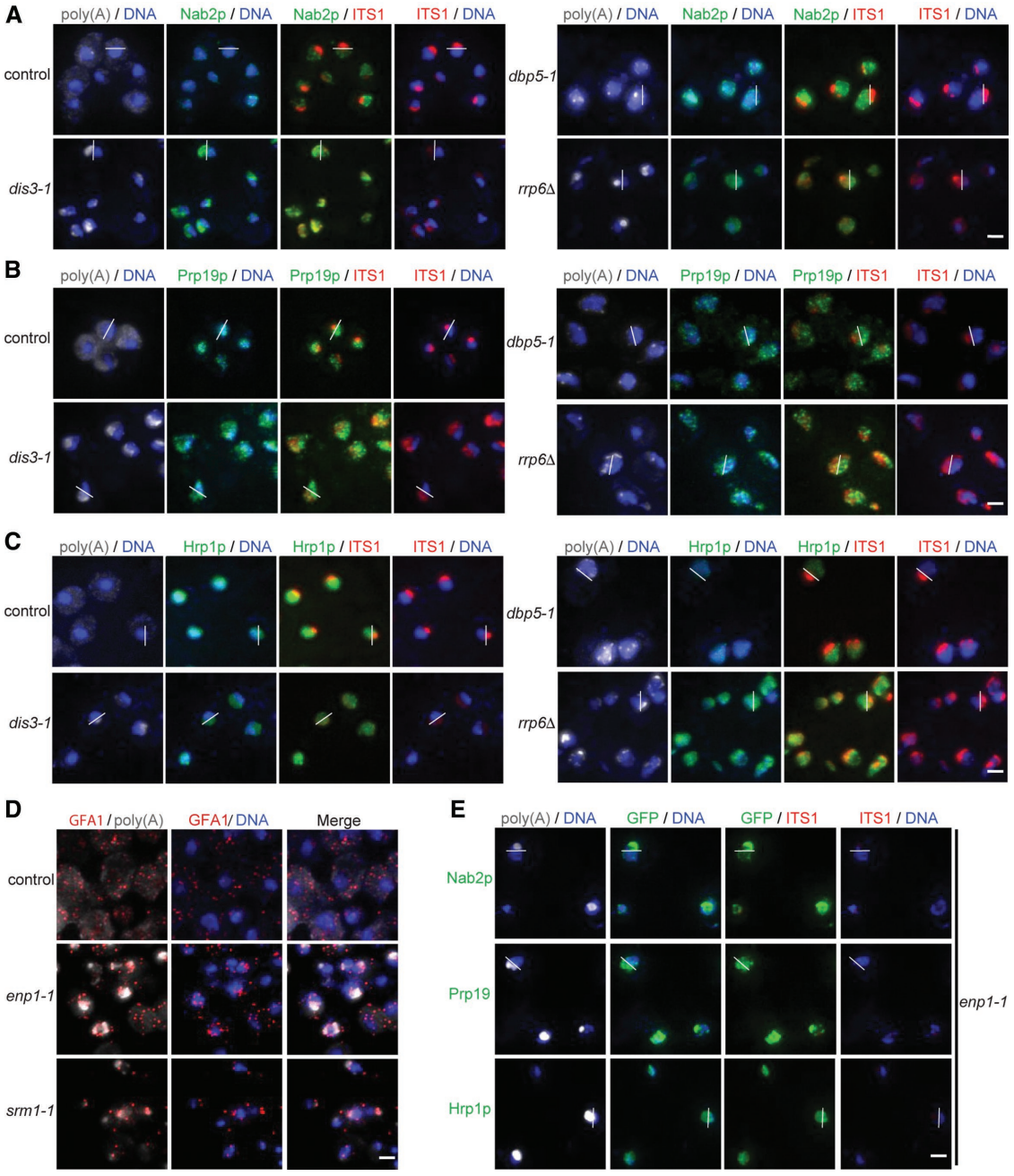

FIGURE 6: Nucleolar enrichment of mRNP-associated proteins in exosome mutants. (A–C, E) Representative images showing localization of Nab2p-GFP, Prp19p-GFP, or Hrp1p-GFP (green) in control (*ura10*Δ), *dbp5-1*, *dis3-1*, *rrp6*Δ, or *enp1-1* strains compared with poly(A)-RNA (gray), *ITS1* (red), and DAPI (blue) after 3 h at 37°C. A white line has been added to one cell in each image to denote the border between DAPI and *ITS1* signals and aid in comparisons. (D) Representative images showing *GFA1* mRNA (red) localization in control (*ura10*Δ), *enp1-1*, and *srm1-ts* strains compared with poly(A)-RNA (gray) and DAPI (blue) after 3 h at 37°C. Scale bars, 1 μm.

without discrete foci) overlapping the DAPI stain, often accompanied by disrupted nucleoli (Figure 1 and Table 1). These mutants further displayed an increased proportion of mRNAs near the nuclear periphery and NPCs (Figure 3). This suggests that within class A mutants, mRNPs accumulated at or near nuclear pore complexes due to failures in NPC-mediated export, which is consistent with the known function of these factors (Table 1). In support of the smFISH observations and data interpretation, delays in export at the nuclear periphery have been observed using live-cell imaging techniques for mutants of *DBP5*, *MEX67*, NAB2, and the Nups *MLP1/2* (Hodge *et al.*, 2011; Saroufim *et al.*, 2015; Smith *et al.*, 2015). Of the class A mutants, *prp2-1* showed a transcript-specific block of mRNA export with the *ACT1* mRNA localized near the nuclear periphery but not another mRNA that lacked an intron (Figures 2 and 3). This observation is consistent with the description of NPC-dependent quality control mechanisms that prevent the export of immature mRNAs, which include pre-mRNAs (Galy *et al.*, 2004; Palancade *et al.*, 2005; Iglesias *et al.*, 2010; Hackmann *et al.*, 2014).

Class B mutants, similar to class A, showed a diffuse poly(A)-RNA distribution (with or without discrete foci) overlapping the DAPI stain

(see *rsp5-3*, Figure 1) but differed in that mRNAs were retained at or near gene transcription sites (Figure 4 and Supplemental Data). Class B mutants included *RSP5, PTA1*, and *CLP1*, which are known to be involved in 3′-end processing (Minvielle-Sebastia *et al.*, 1997; Preker *et al.*, 1997; Zhao *et al.*, 1999; Gwizdek *et al.*, 2005) and could be expected to retain mRNAs at transcription sites due to defects in mRNA biogenesis similar to other mutants affecting cotranscriptional processing (Hilleren *et al.*, 2001; Jensen *et al.*, 2001; Libri *et al.*, 2002; Zenklusen *et al.*, 2002; Thomsen *et al.*, 2008). Ldb19p is a known regulator of Rsp5p in endocytosis (Lin *et al.*, 2008) and was also found to accumulate mRNAs near transcription sites when mutated, like *rsp5-3* (Figure 4). The functional relationship between Ldb19p and Rsp5p with the shared mRNA-processing defects suggests that Ldb19p also regulates the nuclear function of Rsp5p. In support of a nuclear role for Ldb19p, we were able to detect GFP-Ldbp19p in the nucleus when overexpressed from a GAL promoter in an *xpo1-1* mutant that disrupts nucleocytoplasmic transport (Supplemental Figure S2).

Unexpectedly, the majority of class B mutants isolated in our screen (9 of 15) were linked to chromosome segregation and cell division. A previous report noted that mutants affecting chromosome segregation in *S. cerevisiae* displayed poly(A)-RNA accumulation, which was dependent on ongoing cell division (Cole *et al.*, 2002). Given the requirement for ongoing cell division, the large number of chromosome segregation mutants with a class B phenotype, and the fact that these mutants show defects in <25% of cells after 3 h at nonpermissive temperature (Table 1), it is likely that these defects are related to improper chromosome segregation. This could occur through the random loss of genetic material that encodes any one of the many factors involved in mRNA biogenesis, which would be expected to give rise to variable phenotypes, depending on the processing event affected. However, when poly(A)-RNA accumulated in these mutants it was associated with mRNAs appearing at transcription sites and disruption of the nucleolus (Figures 1 and 4 and Supplemental Data). A possible explanation for this more constant phenotype is that specific chromosomes or regions of DNA are repeatedly lost in these mutants and this gives rise to the class B defect due to the specific gene(s) being affected. Alternatively, it has been reported that aneuploid states involving different chromosome imbalances in *S. cerevisiae* result in a set of common cellular characteristics (Torres *et al.*, 2007; Sheltzer *et al.*, 2012), which class B mRNA export phenotypes could exemplify. Although the molecular details are unknown, a recent screen for mutants that alter tRNA processing (Wu *et al.*, 2015) did not report a defect for any chromosome segregation mutants and had only two genes (*NUP133* and *RSP5*) in common with the class B mutants identified here. This lack of overlap hints at a more direct relationship between mRNA export and chromosome segregation; as it would be expected that both mRNA and tRNA processing would be equally susceptible to disruption by random chromosome segregation errors.

Finally, class C mutants displayed poly(A)-RNA accumulation next to the DAPI stain with or adjacent to the nucleolus (based on *ITS1*) and an increased frequency of mRNAs within this compartment (Figures 1, 5, and 6 and Supplemental Data). Many of these mutants are involved in RNA processing and surveillance as components of the exosome and TRAMP complexes, which raises the possibility that the detected mRNAs are aberrant and only become detectable due to a loss of surveillance and decay activities. However, we did not detect an increase in the number of *GFA1* transcripts in these mutants (Table 1), which may be expected if these were common products of transcription that are normally degraded. By using probes against the GFP coding sequence at the 3′ end of an mRNA (Figure 5), we also observed nucleolar mRNA accumulation, suggesting that these transcripts are near full length and not the product of early transcript termination events. Other mutants (e.g., *enp1-1* and *srm1-ts*) that are not part of the decay machinery caused similar mRNA localization phenotypes, suggesting that nucleolar mRNAs are not solely detectable in mutants of the RNA surveillance machinery.

In addition to mRNAs, we also observed enrichment of mRNP-associated factors within the nucleolus in class C mutants (Figures 6). The redistribution of mRNP-associated factors may occur as constituents of mRNPs present within the nucleolus, but it is also possible that poly(A)-RNA binding proteins, such as Nab2p (Anderson *et al.*, 1993), localize to the nucleolus due to promiscuous binding of the protein to accumulated poly(A)-RNA. The latter would effectively deplete the activities of poly(A)-RNA binding proteins, which include mRNA export adaptors, and provide a mechanism by which class C mutants with various cellular functions cause the same terminal phenotype. The heat shock–induced transcript SSA4, the localized mRNA *ASH1*, and *PHO84* antisense RNA have also been reported to enter the nucleolus (Brodsky and Silver, 2000; Thomsen, 2003; Carneiro *et al.*, 2007; Du *et al.*, 2008; Castelnuovo *et al.*, 2013), and mRNAs have recently been observed to transit through the nucleolus for export in live cells (Saroufim *et al.*, 2015). Further study is needed to address how often mRNAs enter the nucleolus during normal mRNA biogenesis, the functional significance of this event, and the molecular mechanism(s) facilitating nucleolar localization.

Nuclear homeostasis and mRNA biogenesis

Disruption of different nuclear processes resulted in classes A–C of mRNA biogenesis defects. We envision this occurring by multiple mechanisms: 1) directly as a result of mutation in a factor involved in mRNA biogenesis and export, 2) by activating quality control mechanisms that retain immature/aberrant mRNPs, and 3) due to changes in nuclear structure/function that result in inefficiencies and failures in mRNA biogenesis and export. The first two mechanisms are exemplified by the *mex67-5* mutation, as it is well established that Mex67p functions directly in mRNA export at NPCs (Segref *et al.*, 1997; Santos-Rosa *et al.*, 1998; Hurt *et al.*, 2000; Sträßer *et al.*, 2000; Lund and Guthrie, 2005; Smith *et al.*, 2015), and a quality control mechanism was described to protect cells during loss of Mex67p function by retaining mRNAs at transcription sites (Kallehauge *et al.*, 2012). Moreover, both mechanisms are highlighted by our smFISH data through the observation of mRNAs that accumulated near the nuclear periphery (e.g., export failure) and the approximately eightfold increase in transcription site foci (e.g., retention) in the *mex67-5* strain (Figure 2 and Supplemental Data). Similar quality control mechanisms have been described in other mutants to cause mRNAs to be retained near transcription sites and at NPCs to prevent export of pre-mRNAs and aberrant mRNPs (Hilleren *et al.*, 2001; Libri *et al.*, 2002; Galy *et al.*, 2004; Palancade *et al.*, 2005; Rougemaille *et al.*, 2008; Saguez *et al.*, 2008; Iglesias *et al.*, 2010; Hackmann *et al.*, 2014), which together may explain many of the observed localization patterns in class A and B mutants.

The third mechanism leading to mRNA biogenesis and export defects likely operates at the systems level and is represented by *srm1-ts*, *enp1-1*, and the many mutants that affect chromosome segregation and exosome function. In these cases, altering nucleocytoplasmic transport and various aspects of RNA biogenesis and inducing aneuploidy would alter nuclear homeostasis, and, in turn, disturb mRNA biogenesis and export. For example, the *enp1-1*

mutation induced strong poly(A)-RNA accumulation in the nucleolus and redistribution of mRNA processing factors to this compartment (Figure 6), which likely affects mRNA processing and export by making these essential factors limiting. This relationship has also been observed to work in reverse, with mRNA export defects causing nucleolar disruption (Kadowaki *et al.*, 1994b; Dockendorff *et al.*, 1997; Segref *et al.*, 1997; Thomsen *et al.*, 2008). In this way, *enp1-1* (and other such mutants) function by perturbing overall nuclear homeostasis and would not be considered an mRNA processing or export factor per se.

Within this paradigm of system-level perturbations, how chromosome segregation mutants affect the cell and cause specific mRNA processing and export defects remains to be determined. We find it noteworthy that aneuploidy is known to alter tumorigenesis through mechanisms that include changes in gene expression (Gordon *et al.*, 2012; Holland and Cleveland, 2012; Santaguida and Amon, 2015; Dürrbaum and Storchová, 2016), and our work highlights the fact that many chromosome segregation mutants cause the accumulation of mRNAs at transcription sites, which provides one mechanism by which this may occur. Although these types of relationships could be casually termed as indirect, these system-level perturbations are important to understand because it is likely that disease states arise from mutation(s) due to both the specific process affected by the mutation and the system-level changes this in turn induces.

MATERIALS AND METHODS

Yeast strains

Strains constructed for this study are listed in the Supplemental Data or were taken directly from mutant collections (Ben-Aroya *et al.*, 2008; Breslow *et al.*, 2008; Li *et al.*, 2011). Strains with genome-encoded, GFP-tagged NOP56, NAB2, PRP19, and HRP1 were generated by amplifying each gene with the GFP::HIS3MX6 cassette plus ~300 base pairs of flanking sequence directly from the yeast GFP collection (Huh *et al.*, 2003). The resulting PCR product was transformed into yeast to integrate the GFP tag into the yeast genome (Gietz *et al.*, 1992). Deletion strains were made by homologous recombination with a selectable marker made by PCR (Longtine *et al.*, 1998). NDC1-yeGFP and GAL1-GFP-LDB19 strains were generated by transforming a PCR product with homology to the gene locus made from pKT148 (Sheff and Thorn, 2004) and pFA6a-His3MX6-PGAL1-GFP (Longtine *et al.*, 1998), respectively. The NOP56-GFP plasmid (pBM461) was made by cloning NOP56-GFP with ~400 base pairs of promoter sequence from the yeast GFP collection (Huh *et al.*, 2003) into pRS313 (Sikorski and Hieter, 1989) using *Xho*I and *Not*I sites introduced by PCR. Tagging of the ACT1 locus with a lacO array was performed in a wild-type strain as previously described using pSR13 and pAFS78 (Straight *et al.*, 1996; Rohner *et al.*, 2008) into which mutant alleles (i.e., LDB19, SLI15, and SPC24) were introduced by transformation of a PCR product. Rescue plasmids were taken from the Yeast ORF Collection (e.g., *CEP3*, *ENP1*, *MPS1*, and *PRP2*; Gelperin *et al.*, 2005), generated by cloning the gene (e.g., *ALR1*, *CLP1*, and *RRP43*) ± 500 base pairs of flanking sequence into pRS41N using *Sac*I and *Hin*dIII sites introduced by PCR, or obtained from the laboratory of Vivien Measday (e.g., *CBF2* and *IPL1*) or Doug Koshland (*SMC1*, *SMC3*, and *SMC4*). All primer sequences are available upon request.

Screen for poly(A)-RNA accumulation

Yeast strains from mutant collections (Ben-Aroya *et al.*, 2008; Breslow *et al.*, 2008; Li *et al.*, 2011) were grown in yeast extract/peptone/dextrose into log phase and then shifted directly to 37°C for 3 h. After temperature shift, cells were fixed for 15 min using 5% formaldehyde, and poly(A)-RNA was detected by FISH using an fluorescein isothiocyanate–labeled oligo-dT probe (Cole *et al.*, 2002). After hybridization of the probe and washing steps, mounting medium with DAPI was applied to each sample and a coverslip was affixed. Imaging was performed on an Olympus IX81 microscope with 100× oil immersion objective (numerical aperture [NA] 1.4) controlled by MetaMorph software (Molecular Devices, Sunnyvale, CA) using identical exposure settings. During each day of screening, *ura10*Δ, *mex67-5*, and *dbp5-1* strains were included as controls to ensure consistency in the FISH procedure. Imaging data (>200 cells) were used to visually score nuclear accumulation of poly(A)-RNA, with mutants showing evidence of accumulation being validated in triplicate. The identity of each strain found to accumulate poly(A)-RNA was subsequently verified by PCR.

Gene-specific FISH

mRNA transcripts were detected using a mixture of up to 48 fluorescently labeled gene probes of 20 nucleotides in length (Biosearch Technologies, Petaluma, CA) with a modified oligo-dT FISH procedure (Amberg *et al.*, 1993). Probe sequences used for each transcript are listed in the Supplemental Data. Briefly, cells were fixed with 5% formaldehyde for 15 min at 37°C, washed with buffer A (0.1 M potassium phosphate, pH 6.5, and 0.5 mM $MgCl_2$), and treated with Zymolyase (250 µg/ml) in buffer B (0.1 M potassium phosphate, pH 6.5, 0.5 mM $MgCl_2$, and 1.2M sorbitol) for 35 min at 37°C. Spheroplasted cells were spotted on poly-L-lysine–coated slides, incubated for 10 min, washed with buffer A to remove unattached cells, permeabilized in cold methanol for 6 min and acetone for 30 s, and allowed to air dry. Cells were rehydrated with hybridization solution (5× SSC [saline-sodium citrate buffer], 5× Denhardt's solution, 0.1% Tween 20, 0.01 mg/ml single-stranded DNA, 0.02 mg/ml *Escherichia coli* tRNA, and 10 mM vanadyl ribonucleoside complex) for 5 min and incubated with fresh hybridization buffer for at least 1 h at 37°C. Hybridization buffer with 1 ng of fluorescein-labeled LNA oligo-dT probe (Exiqon, Woburn, MA), 20 ng of Quasar 570–labeled mRNA probe, and/or 4 ng of Quasar 670–labeled ITS1 probe was added and incubated overnight (~14 h) at 37°C in a humidity chamber. The next day, cells were washed sequentially with 2× SSC, 1× SSC, 0.5× SSC, and 2× phosphate-buffered saline for 5 min at room temperature, and after the final wash, slides were dipped into 100% ethanol for 10 s and air dried, mounting medium with DAPI was applied to each sample, and a coverslip was affixed. Imaging was performed on a DeltaVision Elite microscope system equipped with a front-illuminated scientific complementary metal-oxide-semiconductor (sCMOS) camera driven by Softworx 6 (GE Healthcare, Piscataway, NJ) using an Olympus 60×/1.42 NA oil objective. Image analysis was performed in FIJI (Schindelin *et al.*, 2012), with each three-dimensional smFISH data set being reduced to a single maximum *Z*-projection. mRNA FISH signals were identified as single points within FIJI using noise tolerances set for each individual image and/or smFISH experiment to minimize the detection of false spots and compensate for sample variability. Masks of DAPI and *ITS1* signals were used to quantify the number of mRNAs within these compartments and determine the number of cells within the image being analyzed. Average transcript number per cell was determined from each image, given the number of transcripts and nuclei counted. In control and most mutant strains, foci varied in intensity within a small range and were therefore counted as single transcripts. Bright nuclear foci were apparent in some mutants, but these were counted as single transcripts. This approach was taken for three reasons: 1) where tested, these foci were near transcription

sites, suggesting that they were not mature transcripts or were not released from the site of transcription, 2) the distribution of smFISH probes across the entire length of the mRNA did not allow the differentiation of multiple short transcripts from a full-length mRNA, and 3) these bright foci were generally rare.

Imaging mRNA processing factors

Yeast strains carrying integrated GFP reporters were grown in selective media overnight at room temperature into log phase and shifted directly to 37°C for 3 h. After temperature shift, cells were fixed for 15 min using 4% paraformaldehyde, and poly(A)-RNA was detected using 2 ng of TYE 563–labeled LNA oligo-dT probe (Exiqon) and 4 ng of Quasar 670–labeled ITS1 probe (Biosearch Technologies) by FISH (Cole *et al.*, 2002). After the final wash, slides were dipped in 100% ethanol for 10 s and air dried, mounting medium with DAPI was then applied to each sample, and a coverslip was affixed. Imaging was performed on a DeltaVision Elite microscope system equipped with a front-illuminated sCMOS camera driven by Softworx 6 using an Olympus 60×/1.42 NA oil objective. Image analysis was performed in FIJI (Schindelin *et al.*, 2012).

ACKNOWLEDGMENTS

We thank David Grünwald, Phil Hieter, Doug Koshland, Vivien Measday, Marlene Oeffinger, Karsten Weis, Richard Wozniak, and Daniel Zenklusen for reagents, protocols, and/or helpful discussions. We thank Benedict Yong, Caitlin Porter, and Iris Unterweger for help on the initial screening of mutants and members of the Wozniak and Montpetit laboratories for their support. This research was undertaken, in part, thanks to funding from the Canadian Institutes of Health Research (MOP130231), the Natural Sciences and Engineering Research Council of Canada (RGPIN 435380), the Canada Foundation for Innovation (31271), and the Canada Research Chairs Program.

REFERENCES

Allmang C, Petfalski E, Podtelejnikov A, Mann M, Tollervey D, Mitchell P (1999). The yeast exosome and human PM-Scl are related complexes of 3′ right-arrow 5′ exonucleases. Genes Dev 13, 2148–2158.

Amberg DC, Fleischmann M, Stagljar I, Cole CN, Aebi M (1993). Nuclear PRP20 protein is required for mRNA export. EMBO J 12, 233–241.

Amberg DC, Goldstein AL, Cole CN (1992). Isolation and characterization of RAT1: an essential gene of Saccharomyces cerevisiae required for the efficient nucleocytoplasmic trafficking of mRNA. Genes Dev 6, 1173–1189.

Anderson JT, Wilson SM, Datar KV, Swanson MS (1993). NAB2: a yeast nuclear polyadenylated RNA-binding protein essential for cell viability. Mol Cell Biol 13, 2730–2741.

Belgareh-Touzé N, Léon S, Erpapazoglou Z, Stawiecka-Mirota M, Urban-Grimal D, Haguenauer-Tsapis R (2008). Versatile role of the yeast ubiquitin ligase Rsp5p in intracellular trafficking. Biochem Soc Trans 36, 791–796.

Ben-Aroya S, Coombes C, Kwok T, O'Donnell KA, Boeke JD, Hieter P (2008). Toward a comprehensive temperature-sensitive mutant repository of the essential genes of Saccharomyces cerevisiae. Mol Cell 30, 248–258.

Björk P, Wieslander L (2014). Mechanisms of mRNA export. Semin Cell Dev Biol 32, 47–54.

Bonneau F, Basquin J, Ebert J, Lorentzen E, Conti E (2009). The yeast exosome functions as a macromolecular cage to channel RNA substrates for degradation. Cell 139, 547–559.

Bonnet A, Palancade B (2014). Regulation of mRNA trafficking by nuclear pore complexes. Genes (Basel) 5, 767–791.

Bose T, Lee KK, Lu S, Xu B, Harris B, Slaughter B, Unruh J, Garrett A, McDowell W, Bo A, *et al.* (2012). Cohesin proteins promote ribosomal RNA production and protein translation in yeast and human cells. PLoS Genet 8, e1002749.

Breslow DK, Cameron DM, Collins SR, Schuldiner M, Stewart-Ornstein J, Newman HW, Braun S, Madhani HD, Krogan NJ, Weissman JS (2008). A comprehensive strategy enabling high-resolution functional analysis of the yeast genome. Nat Methods 5, 711–718.

Briggs MW, Burkard KT, Butler JS (1998). Rrp6p, the yeast homologue of the human PM-Scl 100-kDa autoantigen, is essential for efficient 5.8 S rRNA 3′ end formation. J Biol Chem 273, 13255–13263.

Brodsky AS, Silver PA (2000). Pre-mRNA processing factors are required for nuclear export. RNA 6, 1737–1749.

Carneiro T, Carvalho C, Braga J, Rino J, Milligan L, Tollervey D, Carmo-Fonseca M (2007). Depletion of the yeast nuclear exosome subunit Rrp6 results in accumulation of polyadenylated RNAs in a discrete domain within the nucleolus. Mol Cell Biol 27, 4157–4165.

Castelnuovo M, Rahman S, Guffanti E, Infantino V, Stutz F, Zenklusen D (2013). Bimodal expression of PHO84 is modulated by early termination of antisense transcription. Nat Struct Mol Biol 20, 851–858.

Chen W, Bucaria J, Band DA, Sutton A, Sternglanz R (2003). Enp1, a yeast protein associated with U3 and U14 snoRNAs, is required for pre-rRNA processing and 40S subunit synthesis. Nucleic Acids Res 31, 690–699.

Chlebowski A, Lubas M, Jensen TH, Dziembowski A (2013). RNA decay machines: the exosome. Biochim Biophys Acta 1829, 552–560.

Cole CN, Heath CV, Hodge CA, Hammell CM, Amberg DC (2002). Analysis of RNA export. Methods Enzymol 351, 568–587.

D'Amours D, Stegmeier F, Amon A (2004). Cdc14 and condensin control the dissolution of cohesin-independent chromosome linkages at repeated DNA. Cell 117, 455–469.

David L, Huber W, Granovskaia M, Toedling J, Palm CJ, Bofkin L, Jones T, Davis RW, Steinmetz LM (2006). A high-resolution map of transcription in the yeast genome. Proc Natl Acad Sci USA 103, 5320–5325.

Davis CA, Ares M (2006). Accumulation of unstable promoter-associated transcripts upon loss of the nuclear exosome subunit Rrp6p in Saccharomyces cerevisiae. Proc Natl Acad Sci USA 103, 3262–3267.

de Bruyn Kops A, Guthrie C (2001). An essential nuclear envelope integral membrane protein, Brr6p, required for nuclear transport. EMBO J 20, 4183–4193.

Del Priore V, Snay CA, Bahr A, Cole CN (1996). The product of the Saccharomyces cerevisiae RSS1 gene, identified as a high-copy suppressor of the rat7-1 temperature-sensitive allele of the RAT7/NUP159 nucleoporin, is required for efficient mRNA export. Mol Biol Cell 7, 1601–1621.

Dockendorff T, Heath C, Goldstein A, Snay C, Cole C (1997). C-terminal truncations of the yeast nucleoporin Nup145p produce a rapid temperature-conditional mRNA export defect and alterations to nuclear structure. Mol Cell Biol 17, 906–920 [correction published in Mol Cell Biol (1997). 17, 2347–2350].

Doye VR, Wepf R, Hurt EC (1994). A novel nuclear pore protein Nup133p with distinct roles in poly(A)+RNA transport and nuclear pore distribution. EMBO J 13, 6062–6075.

Du T-G, Jellbauer S, Müller M, Schmid M, Niessing D, Jansen R-P (2008). Nuclear transit of the RNA-binding protein She2 is required for translational control of localized ASH1 mRNA. EMBO Rep 9, 781–787.

Dürrbaum M, Storchová Z (2016). Effects of aneuploidy on gene expression: implications for cancer. FEBS J 283, 791–802.

Eberle AB, Visa N (2014). Quality control of mRNP biogenesis: networking at the transcription site. Semin Cell Dev Biol 32, 37–46.

Fabre E, Boelens WC, Wimmer C, Mattaj IW, Hurt EC (1994). Nup145p is required for nuclear export of mRNA and binds homopolymeric RNA in vitro via a novel conserved motif. Cell 78, 275–289.

Freeman L (2000). The condensin complex governs chromosome condensation and mitotic transmission of rDNA. J Cell Biol 149, 811–824.

Galy V, Gadal O, Fromont-Racine M, Romano A, Jacquier A, Nehrbass U (2004). Nuclear retention of unspliced mRNAs in yeast is mediated by perinuclear Mlp1. Cell 116, 63–73.

Gautier T, Bergès T, Tollervey D, Hurt E (1997). Nucleolar KKE/D repeat proteins Nop56p and Nop58p interact with Nop1p and are required for ribosome biogenesis. Mol Cell Biol 17, 7088–7098.

Gelperin DM, White MA, Wilkinson ML, Kon Y, Kung LA, Wise KJ, Lopez-Hoyo N, Jiang L, Piccirillo S, Yu H, *et al.* (2005). Biochemical and genetic analysis of the yeast proteome with a movable ORF collection. Genes Dev 19, 2816–2826.

Gietz D, St Jean A, Woods RA, Schiestl RH (1992). Improved method for high efficiency transformation of intact yeast cells. Nucleic Acids Res 20, 1425.

Gordon DJ, Resio B, Pellman D (2012). Causes and consequences of aneuploidy in cancer. Nat Rev Genet 13, 189–203.

Gorsch LC, Dockendorff TC, Cole CN (1995). A conditional allele of the novel repeat-containing yeast nucleoporin RAT7/NUP159 causes both

rapid cessation of mRNA export and reversible clustering of nuclear pore complexes. J Cell Biol 129, 939–955.
Gudipati RK, Xu Z, Lebreton A, Séraphin B, Steinmetz LM, Jacquier A, Libri D (2012). Extensive degradation of RNA precursors by the exosome in wild-type cells. Mol Cell 48, 409–421.
Gwizdek C, Hobeika M, Kus B, Ossareh-Nazari B, Dargemont C, Rodriguez MS (2005). The mRNA nuclear export factor Hpr1 is regulated by Rsp5-mediated ubiquitylation. J Biol Chem 280, 13401–13405.
Hackmann A, Wu H, Schneider U-M, Meyer K, Jung K, Krebber H (2014). Quality control of spliced mRNAs requires the shuttling SR proteins Gbp2 and Hrb1. Nat Commun 5, 3123.
Hammell CM, Gross S, Zenklusen D, Heath CV, Stutz F, Moore C, Cole CN (2002). Coupling of termination, 3′ processing, and mRNA export. Mol Cell Biol 22, 6441–6457.
Harris B, Bose T, Lee KK, Wang F, Lu S, Ross RT, Zhang Y, French SL, Beyer AL, Slaughter BD, *et al.* (2014). Cohesion promotes nucleolar structure and function. Mol Biol Cell 25, 337–346.
Hieronymus H, Yu MC, Silver PA (2004). Genome-wide mRNA surveillance is coupled to mRNA export. Genes Dev 18, 2652–2662.
Hilleren P, McCarthy T, Rosbash M, Parker R, Jensen TH (2001). Quality control of mRNA 3′-end processing is linked to the nuclear exosome. Nature 413, 538–542.
Hodge CA, Choudhary V, Wolyniak MJ, Scarcelli JJ, Schneiter R, Cole CN (2010). Integral membrane proteins Brr6 and Apq12 link assembly of the nuclear pore complex to lipid homeostasis in the endoplasmic reticulum. J Cell Sci 123, 141–151.
Hodge CA, Tran EJ, Noble KN, Alcazar-Roman AR, Ben-Yishay R, Scarcelli JJ, Folkmann AW, Shav-Tal Y, Wente SR, Cole CN (2011). The Dbp5 cycle at the nuclear pore complex during mRNA export I: Dbp5 mutants with defects in RNA binding and ATP hydrolysis define key steps for Nup159 and Gle1. Genes Dev 25, 1052–1064.
Holland AJ, Cleveland DW (2012). Losing balance: the origin and impact of aneuploidy in cancer. EMBO Rep 13, 501–514.
Houalla R, Devaux F, Fatica A, Kufel J, Barrass D, Torchet C, Tollervey D (2006). Microarray detection of novel nuclear RNA substrates for the exosome. Yeast 23, 439–454.
Houseley J, Tollervey D (2009). The many pathways of RNA degradation. Cell 136, 763–776.
Huh W-KK, Falvo JV, Gerke LC, Carroll AS, Howson RW, Weissman JS, O'Shea EK (2003). Global analysis of protein localization in budding yeast. Nature 425, 686–691.
Hurt E, Strasser K, Segref A, Bailer S, Schlaich N, Presutti C, Tollervey D, Jansen R (2000). Mex67p mediates nuclear export of a variety of RNA polymerase II transcripts. J Biol Chem 275, 8361–8368.
Ideue T, Azad AK, Yoshida J, Matsusaka T, Yanagida M, Ohshima Y, Tani T (2004). The nucleolus is involved in mRNA export from the nucleus in fission yeast. J Cell Sci 117, 2887–2895.
Iglesias N, Tutucci E, Gwizdek C, Vinciguerra P, Von Dach E, Corbett AH, Dargemont C, Stutz F (2010). Ubiquitin-mediated mRNP dynamics and surveillance prior to budding yeast mRNA export. Genes Dev 24, 1927–1938.
Jacobs JS, Anderson AR, Parker RP (1998). The 3′ to 5′ degradation of yeast mRNAs is a general mechanism for mRNA turnover that requires the SKI2 DEVH box protein and 3′ to 5′ exonucleases of the exosome complex. EMBO J 17, 1497–1506.
Jensen TH, Boulay J, Rosbash M, Libri D (2001). The DECD box putative ATPase Sub2p is an early mRNA export factor. Curr Biol 11, 1711–1715.
Kadaba S, Krueger A, Trice T, Krecic AM, Hinnebusch AG, Anderson J (2004). Nuclear surveillance and degradation of hypomodified initiator tRNAMet in S. cerevisiae. Genes Dev 18, 1227–1240.
Kadowaki T, Chen S, Hitomi M, Jacobs E, Kumagai C, Liang S, Schneiter R, Singleton D, Wisniewska J, Tartakoff AM (1994a). Isolation and characterization of Saccharomyces cerevisiae mRNA transport-defective (mtr) mutants. J Cell Biol 126, 649–659 [correction published in J Cell Biol (1994). 126, 1627].
Kadowaki T, Hitomi M, Chen S, Tartakoff AM (1994b). Nuclear mRNA accumulation causes nucleolar fragmentation in yeast mtr2 mutant. Mol Biol Cell 5, 1253–1263.
Kadowaki T, Zhao Y, Tartakoff AM (1992). A conditional yeast mutant deficient in mRNA transport from nucleus to cytoplasm. Proc Natl Acad Sci USA 89, 2312–2316.
Kalam Azad A, Ideue T, Ohshima Y, Tani T (2003). A mutation in the gene involved in sister chromatid separation causes a defect in nuclear mRNA export in fission yeast. Biochem Biophys Res Commun 310, 176–181.
Kaliszewski P, Zoładek T (2008). The role of Rsp5 ubiquitin ligase in regulation of diverse processes in yeast cells. Acta Biochim Pol 55, 649–662.
Kallehauge TB, Robert M-C, Bertrand E, Jensen TH (2012). Nuclear retention prevents premature cytoplasmic appearance of mRNA. Mol Cell 48, 145–152.
Koepp DM, Wong DH, Corbett AH, Silver PA (1996). Dynamic localization of the nuclear import receptor and its interactions with transport factors. J Cell Biol 133, 1163–1176.
Kuai L, Fang F, Butler JS, Sherman F (2004). Polyadenylation of rRNA in Saccharomyces cerevisiae. Proc Natl Acad Sci USA 101, 8581–8586.
LaCava J, Houseley J, Saveanu C, Petfalski E, Thompson E, Jacquier A, Tollervey D (2005). RNA degradation by the exosome is promoted by a nuclear polyadenylation complex. Cell 121, 713–724.
Li Z, Vizeacoumar FJ, Bahr S, Li J, Warringer J, Vizeacoumar FS, Min R, Vandersluis B, Bellay J, Devit M, *et al.* (2011). Systematic exploration of essential yeast gene function with temperature-sensitive mutants. Nat Biotechnol 29, 361–367.
Libri D, Dower K, Boulay J, Thomsen R, Rosbash M, Jensen TH (2002). Interactions between mRNA export commitment, 3′-end quality control, and nuclear degradation. Mol Cell Biol 22, 8254–8266.
Lin CH, MacGurn JA, Chu T, Stefan CJ, Emr SD (2008). Arrestin-related ubiquitin-ligase adaptors regulate endocytosis and protein turnover at the cell surface. Cell 135, 714–725.
Liu Q, Greimann JC, Lima CD (2006). Reconstitution, activities, and structure of the eukaryotic RNA exosome. Cell 127, 1223–1237.
Lone MA, Atkinson AE, Hodge CA, Cottier S, Martínez-Montañés F, Maithel S, Mène-Saffrané L, Cole CN, Schneiter R (2015). Yeast integral membrane proteins Apq12, Brl1, and Brr6 form a complex important for regulation of membrane homeostasis and nuclear pore complex biogenesis. Eukaryot Cell 14, 1217–1227.
Longtine MS, McKenzie A 3rd, Demarini DJ, Shah NG, Wach A, Brachat A, Philippsen P, Pringle JR (1998). Additional modules for versatile and economical PCR-based gene deletion and modification in Saccharomyces cerevisiae. Yeast 14, 953–961.
Lund MK, Guthrie C (2005). The DEAD-box protein Dbp5p is required to dissociate Mex67p from exported mRNPs at the nuclear rim. Mol Cell 20, 645–651.
Lustig AJ, Lin RJ, Abelson J (1986). The yeast RNA gene products are essential for mRNA splicing in vitro. Cell 47, 953–963.
Machín F, Torres-Rosell J, Jarmuz A, Aragón L (2005). Spindle-independent condensation-mediated segregation of yeast ribosomal DNA in late anaphase. J Cell Biol 168, 209–219.
Malet H, Topf M, Clare DK, Ebert J, Bonneau F, Basquin J, Drazkowska K, Tomecki R, Dziembowski A, Conti E, *et al.* (2010). RNA channelling by the eukaryotic exosome. EMBO Rep 11, 936–942.
Minvielle-Sebastia L, Preker PJ, Wiederkehr T, Strahm Y, Keller W (1997). The major yeast poly(A)-binding protein is associated with cleavage factor IA and functions in premessenger RNA 3′-end formation. Proc Natl Acad Sci USA 94, 7897–7902.
Mitchell SF, Parker R (2014). Principles and properties of eukaryotic mRNPs. Mol Cell 54, 547–558.
Mitchell P, Petfalski E, Shevchenko A, Mann M, Tollervey D (1997). The exosome: a conserved eukaryotic RNA processing complex containing multiple 3′→5′ exoribonucleases. Cell 91, 457–466.
Müller-McNicoll M, Neugebauer KM (2013). How cells get the message: dynamic assembly and function of mRNA-protein complexes. Nat Rev Genet 14, 275–287.
Murphy R, Wente SR (1996). An RNA-export mediator with an essential nuclear export signal. Nature 383, 357–360.
Neumann S, Petfalski E, Brügger B, Grosshans H, Wieland F, Tollervey D, Hurt E (2003). Formation and nuclear export of tRNA, rRNA and mRNA is regulated by the ubiquitin ligase Rsp5p. EMBO Rep 4, 1156–1162.
Ng R, Abelson J (1980). Isolation and sequence of the gene for actin in Saccharomyces cerevisiae. Proc Natl Acad Sci USA 77, 3912–3916.
Niño CA, Hérissant L, Babour A, Dargemont C (2013). mRNA nuclear export in yeast. Chem Rev 113, 8523–8545.
Oeffinger M, Montpetit B (2015). Emerging properties of nuclear RNP biogenesis and export. Curr Opin Cell Biol 34, 46–53.
Oeffinger M, Zenklusen D (2012). To the pore and through the pore: a story of mRNA export kinetics. Biochim Biophys Acta 1819, 494–506.
Palancade B, Zuccolo M, Loeillet S, Nicolas A, Doye V (2005). Pml39, a novel protein of the nuclear periphery required for nuclear retention of improper messenger ribonucleoparticles. Mol Biol Cell 16, 5258–5268.
Porrua O, Libri D (2013). RNA quality control in the nucleus: the Angels' share of RNA. Biochim Biophys Acta 1829, 604–611.
Porrua O, Libri D (2015). Transcription termination and the control of the transcriptome: why, where and how to stop. Nat Rev Mol Cell Biol 16, 190–202.

Preker PJ, Ohnacker M, Minvielle-Sebastia L, Keller W (1997). A multisubunit 3′ end processing factor from yeast containing poly(A) polymerase and homologues of the subunits of mammalian cleavage and polyadenylation specificity factor. EMBO J 16, 4727–4737.
Rodriguez MS, Gwizdek C, Haguenauer-Tsapis R, Dargemont C (2003). The HECT ubiquitin ligase Rsp5p is required for proper nuclear export of mRNA in Saccharomyces cerevisiae. Traffic 4, 566–575.
Rohner S, Gasser SM, Meister P (2008). Modules for cloning-free chromatin tagging in Saccharomyces cerevisae. Yeast 25, 235–239.
Rougemaille M, Dieppois G, Kisseleva-Romanova E, Gudipati RK, Lemoine S, Blugeon C, Boulay J, Jensen TH, Stutz F, Devaux F, *et al.* (2008). THO/Sub2p functions to coordinate 3′-end processing with gene-nuclear pore association. Cell 135, 308–321.
Rougemaille M, Gudipati RK, Olesen JR, Thomsen R, Seraphin B, Libri D, Jensen TH (2007). Dissecting mechanisms of nuclear mRNA surveillance in THO/sub2 complex mutants. EMBO J 26, 2317–2326.
Saguez C, Schmid M, Olesen JR, Ghazy MAE-H, Qu X, Poulsen MB, Nasser T, Moore C, Jensen TH (2008). Nuclear mRNA surveillance in THO/sub2 mutants is triggered by inefficient polyadenylation. Mol Cell 31, 91–103.
Saitoh Y-H, Ogawa K, Nishimoto T (2005). Brl1p—a novel nuclear envelope protein required for nuclear transport. Traffic 6, 502–517.
Santaguida S, Amon A (2015). Short- and long-term effects of chromosome mis-segregation and aneuploidy. Nat Rev Mol Cell Biol 16, 473–485.
Santos-Rosa H, Moreno H, Simos G, Segref A, Fahrenkrog B, Pante N, Hurt E (1998). Nuclear mRNA export requires complex formation between Mex67p and Mtr2p at the nuclear pores. Mol Cell Biol 18, 6826–6838.
Saroufim M-A, Bensidoun P, Raymond P, Rahman S, Krause MR, Oeffinger M, Zenklusen D (2015). The nuclear basket mediates perinuclear mRNA scanning in budding yeast. J Cell Biol 211, 1131–1140.
Schindelin J, Arganda-Carreras I, Frise E, Kaynig V, Longair M, Pietzsch T, Preibisch S, Rueden C, Saalfeld S, Schmid B, *et al.* (2012). Fiji: an open-source platform for biological-image analysis. Nat Methods 9, 676–682.
Schneider C, Kudla G, Wlotzka W, Tuck A, Tollervey D (2012). Transcriptome-wide analysis of exosome targets. Mol Cell 48, 422–433.
Schneider C, Tollervey D (2013). Threading the barrel of the RNA exosome. Trends Biochem Sci 38, 485–493.
Segref A, Sharma K, Doye V, Hellwig A, Huber J, Luhrmann R, Hurt E, Lührmann R (1997). Mex67p, a novel factor for nuclear export, binds to both poly(A)+ RNA and nuclear pores. EMBO J 16, 3256–3271.
Sheff MA, Thorn KS (2004). Optimized cassettes for fluorescent protein tagging in Saccharomyces cerevisiae. Yeast 21, 661–670.
Sheltzer JM, Torres EM, Dunham MJ, Amon A (2012). Transcriptional consequences of aneuploidy. Proc Natl Acad Sci USA 109, 12644–12649.
Shiokawa K, Pogo AO (1974). The role of cytoplasmic membranes in controlling the transport of nuclear messenger RNA and initiation of protein synthesis. Proc Natl Acad Sci USA 71, 2658–2662.
Sikorski RS, Hieter P (1989). A system of shuttle vectors and yeast host strains designed for efficient manipulation of DNA in Saccharomyces cerevisiae. Genetics 122, 19–27.
Singh G, Pratt G, Yeo GW, Moore MJ (2015). The clothes make the mRNA: past and present trends in mRNP fashion. Annu Rev Biochem 84, 325–354.
Smith C, Lari A, Derrer CP, Ouwehand A, Rossouw A, Huisman M, Dange T, Hopman M, Joseph A, Zenklusen D, *et al.* (2015). In vivo single-particle imaging of nuclear mRNA export in budding yeast demonstrates an essential role for Mex67p. J Cell Biol 211, 1121–1130.
Snay-Hodge CA, Colot HV, Goldstein AL, Cole CN (1998). Dbp5p/Rat8p is a yeast nuclear pore-associated DEAD-box protein essential for RNA export. EMBO J 17, 2663–2676.
Steinmetz EJ, Conrad NK, Brow DA, Corden JL (2001). RNA-binding protein Nrd1 directs poly(A)-independent 3′-end formation of RNA polymerase II transcripts. Nature 413, 327–331.
Straight AF, Belmont AS, Robinett CC, Murray AW (1996). GFP-tagging of budding yeast chromosomes reveals that protein-protein interactions can mediate sister chromatid cohesion. Curr Biol 6, 1599–1608.
Sträßer K, Baßler J, Hurt E (2000). Binding of the Mex67p/Mtr2p heterodimer to FXFG, GLFG, and FG repeat nucleoporins is essential for nuclear mRNA export. J Cell Biol 150, 695–706.
Sullivan M, Higuchi T, Katis VL, Uhlmann F (2004). Cdc14 phosphatase induces rDNA condensation and resolves cohesin-independent cohesion during budding yeast anaphase. Cell 117, 471–482.
Tachibana T, Imamoto N, Seino H, Nishimoto T, Yoneda Y (1994). Loss of RCC1 leads to suppression of nuclear protein import in living cells. J Biol Chem 269, 24542–24545.
Thomsen R (2003). Localization of nuclear retained mRNAs in Saccharomyces cerevisiae. RNA 9, 1049–1057.
Thomsen R, Saguez C, Nasser T, Jensen TH (2008). General, rapid, and transcription-dependent fragmentation of nucleolar antigens in S. cerevisiae mRNA export mutants. RNA 14, 706–716.
Torres EM, Sokolsky T, Tucker CM, Chan LY, Boselli M, Dunham MJ, Amon A (2007). Effects of aneuploidy on cellular physiology and cell division in haploid yeast. Science 317, 916–924.
Tseng SS, Weaver PL, Liu Y, Hitomi M, Tartakoff AM, Chang TH (1998). Dbp5p, a cytosolic RNA helicase, is required for poly(A)+ RNA export. EMBO J 17, 2651–2662.
Tuck AC, Tollervey D (2013). A transcriptome-wide atlas of RNP composition reveals diverse classes of mRNAs and lncRNAs. Cell 154, 996–1009.
Ursic D, Chinchilla K, Finkel JS, Culbertson MR (2004). Multiple protein/protein and protein/RNA interactions suggest roles for yeast DNA/RNA helicase Sen1p in transcription, transcription-coupled DNA repair and RNA processing. Nucleic Acids Res 32, 2441–2452.
Vanácová S, Wolf J, Martin G, Blank D, Dettwiler S, Friedlein A, Langen H, Keith G, Keller W (2005). A new yeast poly(A) polymerase complex involved in RNA quality control. PLoS Biol 3, e189.
van Hoof A, Lennertz P, Parker R (2000). Yeast exosome mutants accumulate 3′-extended polyadenylated forms of U4 small nuclear RNA and small nucleolar RNAs. Mol Cell Biol 20, 441–452.
Vasiljeva L, Buratowski S (2006). Nrd1 interacts with the nuclear exosome for 3′ processing of RNA polymerase II transcripts. Mol Cell 21, 239–248.
Wasmuth VE, Lima CD (2012). Exo- and endoribonucleolytic activities of yeast cytoplasmic and nuclear RNA exosomes are dependent on the noncatalytic core and central channel. Mol Cell 48, 133–144.
Wente SR, Blobel G (1994). NUP145 encodes a novel yeast glycine-leucine-phenylalanine-glycine (GLFG) nucleoporin required for nuclear envelope structure. J Cell Biol 125, 955–969.
Wente SR, Rout MP (2010). The nuclear pore complex and nuclear transport. Cold Spring Harb Perspect Biol 2, a000562.
Woolford JL, Baserga SJ (2013). Ribosome biogenesis in the yeast Saccharomyces cerevisiae. Genetics 195, 643–681.
Wu J, Bao A, Chatterjee K, Wan Y, Hopper AK (2015). Genome-wide screen uncovers novel pathways for tRNA processing and nuclear-cytoplasmic dynamics. Genes Dev 29, 2633–2644.
Wyers F, Rougemaille M, Badis G, Rousselle J-C, Dufour M-E, Boulay J, Régnault B, Devaux F, Namane A, Séraphin B, *et al.* (2005). Cryptic pol II transcripts are degraded by a nuclear quality control pathway involving a new poly(A) polymerase. Cell 121, 725–737.
Zenklusen D, Vinciguerra P, Wyss JC, Stutz F (2002). Stable mRNP formation and export require cotranscriptional recruitment of the mRNA export factors Yra1p and Sub2p by Hpr1p. Mol Cell Biol 22, 8241–8253.
Zhao J, Kessler M, Helmling S, O'Connor JP, Moore C (1999). Pta1, a component of yeast CF II, is required for both cleavage and poly(A) addition of mRNA precursor. Mol Cell Biol 19, 7733–7740.